

## CHAGAS DISEASE

## A modified drug regimen clears active and dormant trypanosomes in mouse models of Chagas disease

Juan M. Bustamante<sup>1\*</sup>, Fernando Sanchez-Valdez<sup>1,2\*</sup>, Angel M. Padilla<sup>1</sup>, Brooke White<sup>1</sup>, Wei Wang<sup>1</sup>, Rick L. Tarleton<sup>1,3†</sup>Copyright © 2020  
The Authors, some  
rights reserved;  
exclusive licensee  
American Association  
for the Advancement  
of Science. No claim  
to original U.S.  
Government Works

A major contributor to treatment failure in Chagas disease, caused by infection with the protozoan parasite *Trypanosoma cruzi*, is that current treatment regimens do not address the drug insensitivity of transiently dormant *T. cruzi* amastigotes. Here, we demonstrated that use of a currently available drug in a modified treatment regimen of higher individual doses, given less frequently over an extended treatment period, could consistently extinguish *T. cruzi* infection in three mouse models of Chagas disease. Once per week administration of benznidazole at a dose 2.5 to 5 times the standard daily dose rapidly eliminated actively replicating parasites and ultimately eradicated the residual, transiently dormant parasite population in mice. This outcome was initially confirmed in “difficult to cure” mouse infection models using immunological, parasitological, and molecular biological approaches and ultimately corroborated by whole organ analysis of optically clarified tissues using light sheet fluorescence microscopy (LSFM). This tool was effective for monitoring pathogen load in intact organs, including detection of individual dormant parasites, and for assessing treatment outcomes. LSFM-based analysis also suggested that dormant amastigotes of *T. cruzi* may not be fully resistant to trypanocidal compounds such as benznidazole. Collectively, these studies provide important information on the phenomenon of dormancy in *T. cruzi* infection in mice, demonstrate methods to therapeutically override dormancy using a currently available drug, and provide methods to monitor alternative therapeutic approaches for this, and possibly other, low-density infectious agents.

## INTRODUCTION

Chagas disease, caused by the protozoan parasite *Trypanosoma cruzi*, is a potentially life-threatening infection that currently affects at least 6 million people in the Americas and has spread to non-endemic countries through human migration (1–3). The number of individuals infected with *T. cruzi* continues to increase and is amplified by a widespread failure to apply vector control approaches and the absence of effective vaccines. Furthermore, the disease symptoms are exacerbated by the fact that most infections with *T. cruzi* go undetected and/or untreated. The frontline therapies for *T. cruzi* infection consist of two compounds, benznidazole (BNZ) and nifurtimox (NFX), both of which are associated with adverse events, have unpredictable efficacy, and are administered in an intense, twice-daily regimen for 30 to 60 days (4–6). These attributes lead to treatment interruption in approximately 20% of individuals (6, 7) and contribute to the fact that only ~1% of infected subjects are thought to receive a full course of treatment (8). This situation is particularly dire because *T. cruzi* infection rarely resolves without treatment and often progressively damages critical organs such as the heart, leading to eventual heart failure.

The frequent failure of the standard 30- to 60-day BNZ treatment regimens is paradoxical, given that a single in vivo dose of this compound rapidly reduces parasite load by ~90% (9) and that shortened treatment regimens in experimental animals and humans occasionally are curative (7, 10). One facet of the inconsistency in treatment outcomes is *T. cruzi* strain variation, as some isolates are more resistant to BNZ-induced clearance in vivo (9, 10), despite having similar

sensitivity to BNZ in vitro. There are major gaps in our understanding of the biology of intracellular amastigotes of *T. cruzi*, the targets for drug therapy. *T. cruzi* amastigotes replicate in the cytoplasm of a wide variety of host cell types, but the true tissue distribution in vivo, the kinetics of replication in different host cell and tissue types, and the impact of host factors, including immune effectors, on parasite control and persistence are not known. We recently reported a previously undescribed stage in the intracellular life cycle of *T. cruzi*, transiently dormant, and nonreplicating amastigotes that are resistant to treatment with existing trypanocidal compounds, including BNZ (9). The transition into dormancy by *T. cruzi* amastigotes occurs at a very low frequency and appears to be stochastic and not a response to stressors, including drug exposure. This dormancy phenotype is also transient, with formally dormant amastigotes returning to an active dividing state that is sensitive to drug. Thus, trypanocidal drugs very efficiently kill actively dividing amastigotes but not dormant forms, suggesting that dormancy is a primary cause of the failure of these drugs to achieve consistent parasitological cure in this and perhaps other parasitic infection (11).

These findings reveal a need to rethink drug discovery for Chagas disease. To date, all screens for anti-*T. cruzi* compounds have focused on discovering entities that kill actively dividing/nondormant amastigotes. New screens capable of identifying compounds that can interrupt or reverse dormancy or kill dormant forms are needed. Alternatively, we can ask how we might better apply the existing trypanocidal compounds to overcome dormancy. On the basis of the knowledge that single doses of BNZ are highly toxic for replicating *T. cruzi* and with the assumption that dormancy is time limited, in this study, we have developed and evaluated a longer-term but less-intensive and ultimately drug-sparing BNZ treatment protocol in mice with chronic infections with hard-to-cure isolates of *T. cruzi*. Furthermore, to document the kinetics and impact of this protocol in vivo over time, we established tissue clearing and light sheet

<sup>1</sup>Center for Tropical and Emerging Global Diseases, University of Georgia, Athens, Georgia, USA. <sup>2</sup>Instituto de Patología Experimental, Universidad Nacional de Salta-CONICET, Salta, Argentina. <sup>3</sup>Department of Cellular Biology, University of Georgia, Athens, Georgia, USA.

\*These authors contributed equally to this work.

†Corresponding author. Email: tarleton@uga.edu

fluorescence microscopy (LSFM) methods that allow the quantification of actively replicating and dormant parasites, including single parasites, in intact tissues and organs. Application of these regimens and methodologies provides new insights on dormancy in *T. cruzi* and suggests methods to achieve parasitological cure despite dormancy.

## RESULTS

### Single or multiple intermittent doses of BNZ sustainably reduce parasite load

Following on our new understanding of the resistance of dormant amastigotes to BNZ and other trypanocidal drugs, and solid evidence for the failure of current, intensive drug treatment protocols in Chagas disease, we hypothesized that delivering BNZ over a longer period of time could “outpace” dormancy, killing all actively replicating parasites early in the treatment regimen and eventually clearing all parasites, as the remaining dormant forms gradually emerged over time of treatment. Given the known toxicity of the daily BNZ treatment protocols (6, 12, 13), extending daily dosing for >60 days seemed impractical. However, evidence of the substantial impact of

intermittent dosing once every ~5 days on *T. cruzi* infection in humans and experimental animals (7, 10) provided support for a protocol of less frequent dosing. To examine directly the impact of intermittent dosing on total parasite load, we monitored luciferase-expressing parasites at the site of infection after the standard daily oral dose of BNZ (100 mg/kg) or a fivefold higher dose (Fig. 1A).

Both the 100 and 500 mg/kg BNZ doses reduced parasite numbers by >90% within 1 day after treatment, as expected (Fig. 1, B and C) (9). However, the 500 mg/kg dose had a sustained impact for at least 5 days, whereas parasite numbers in mice treated with 100 mg/kg began to increase within 2 days after treatment. The differential impact of the two BNZ doses on parasite load was confirmed by quantitative polymerase chain reaction (qPCR) detection of parasites in the footpad of wild-type mice 5 days after a single BNZ treatment (Fig. 1D). In both cases, subsequent doses of BNZ drove parasite numbers even lower and two to three doses over ~20 days at either dose were sufficient to reduce parasite load to background (Fig. 1C) in these interferon- $\gamma$  (IFN- $\gamma$ )–deficient mice that are otherwise unable to control infection without drug intervention (14, 15). These results demonstrate that less frequent BNZ dosing has a durable impact on parasite numbers, but the standard dose of 100 mg/kg BNZ

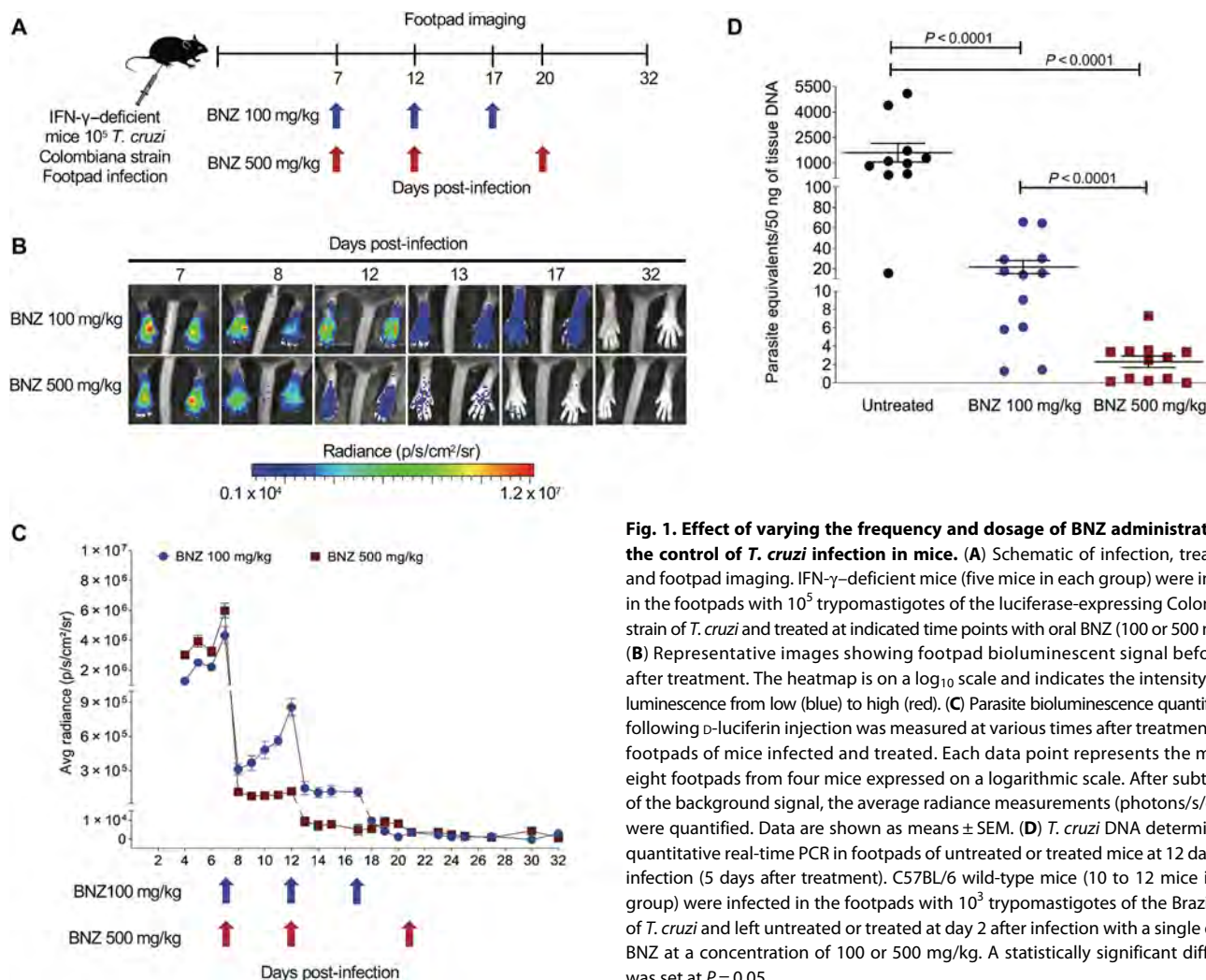


**Fig. 1. Effect of varying the frequency and dosage of BNZ administration on the control of *T. cruzi* infection in mice.** (A) Schematic of infection, treatment, and footpad imaging. IFN- $\gamma$ -deficient mice (five mice in each group) were infected in the footpads with  $10^5$  trypomastigotes of the luciferase-expressing Colombiana strain of *T. cruzi* and treated at indicated time points with oral BNZ (100 or 500 mg/kg). (B) Representative images showing footpad bioluminescent signal before and after treatment. The heatmap is on a log<sub>10</sub> scale and indicates the intensity of bioluminescence from low (blue) to high (red). (C) Parasite bioluminescence quantification following D-luciferin injection was measured at various times after treatment in the footpads of mice infected and treated. Each data point represents the mean of eight footpads from four mice expressed on a logarithmic scale. After subtraction of the background signal, the average radiance measurements (photons/s/cm<sup>2</sup>/sr) were quantified. Data are shown as means  $\pm$  SEM. (D) *T. cruzi* DNA determined by quantitative real-time PCR in footpads of untreated or treated mice at 12 days after infection (5 days after treatment). C57BL/6 wild-type mice (10 to 12 mice in each group) were infected in the footpads with  $10^3$  trypomastigotes of the Brazil strain of *T. cruzi* and left untreated or treated at day 2 after infection with a single dose of BNZ at a concentration of 100 or 500 mg/kg. A statistically significant difference was set at  $P = 0.05$ .

was initially less effective at decreasing and maintaining a reduced parasite load when used intermittently.

### Once-per-week treatment with BNZ achieves parasitological cure

We then carried out a large-scale treatment study using mice chronically infected with the ARC-0704 line, a strain of *T. cruzi* that, like the Colombiana used in the experiments in Fig. 1, is relatively resistant to BNZ-induced cure using the standard 40-day treatment protocol (fig. S1). Mice were treated weekly with either 100 or 500 mg/kg beginning at 120 days after infection, and the length of treatment was not initially defined (an open-ended protocol; Fig. 2A). Because parasite load in mice with chronic *T. cruzi* infection—even without

treatment—is generally assessable only by highly sensitive protocols like qPCR detection of parasite DNA in tissues at necropsy (16, 17), we were unable to measure directly parasite numbers during the course of this treatment study. However, in cured infections, we had previously shown that the memory status of *T. cruzi*-specific CD8<sup>+</sup> T cells, indicating whether they had recently encountered *T. cruzi* antigen, could serve as a dependable indicator of cure (10, 18). Thus, we used the frequency of the interleukin-7 receptor  $\alpha$  (CD127) high, *T. cruzi*-specific CD8<sup>+</sup> T cells (termed *T. cruzi*-specific T<sub>cm</sub>) as a surrogate for parasite load over the treatment course.

Mice receiving weekly doses of BNZ (either 100 or 500 mg/kg) exhibited increased frequencies of CD127<sup>+</sup> *T. cruzi*-specific CD8<sup>+</sup>

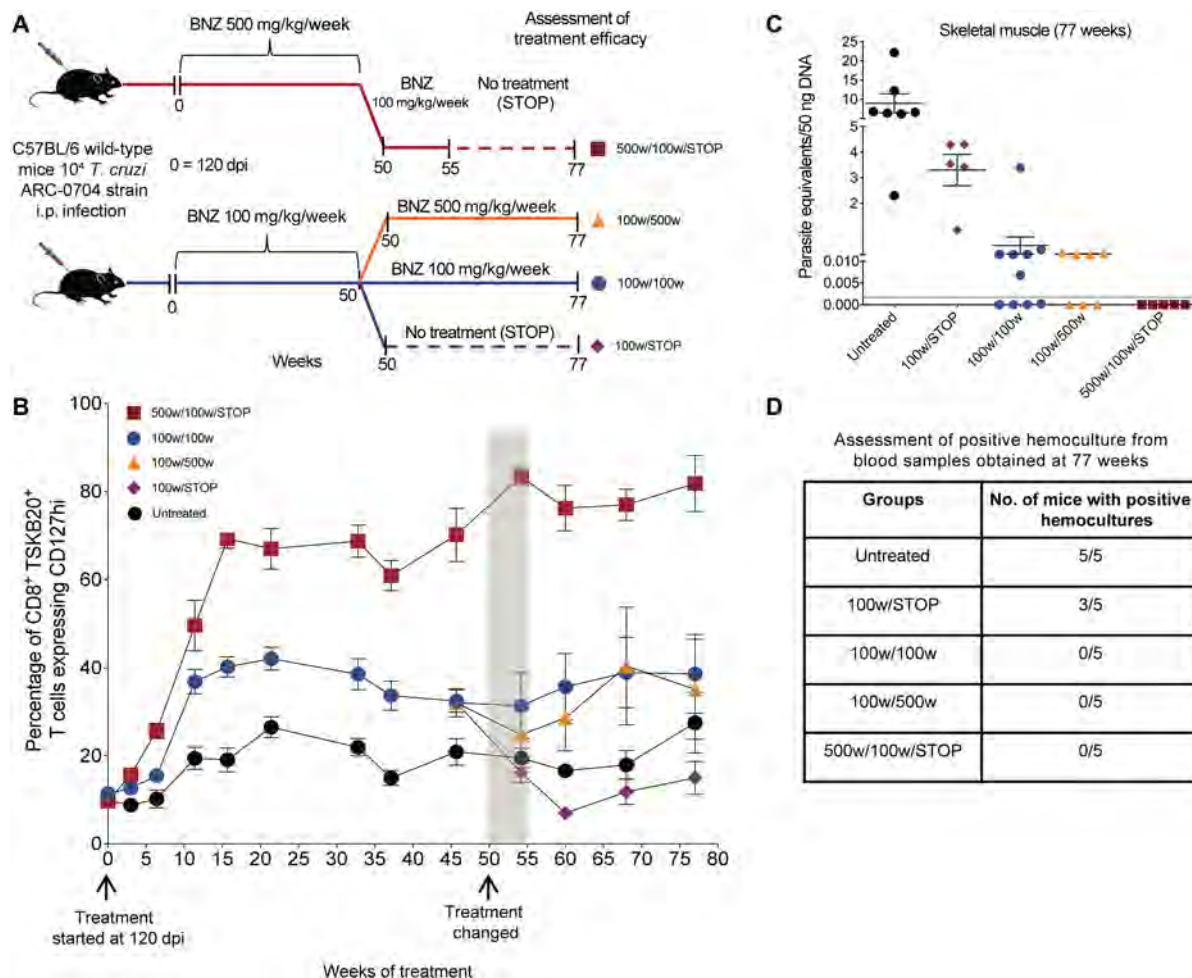


**Fig. 2. A weekly BNZ treatment regimen of 500 mg/kg cures mice chronically infected with *T. cruzi*.** (A) Schematic of infection, treatment, and assessment of treatment efficacy. C57BL/6 wild-type mice (14 to 15 mice in each group) were infected intraperitoneally with  $10^4$  trypomastigotes of the ARC-0704 strain of *T. cruzi* and left untreated or treated weekly, starting at 120 days after infection, with BNZ at a concentration of 100 or 500 mg/kg over 50 weeks. At 50 weeks of treatment, mice treated with 500 mg/kg per week were switched to a regimen of 100 mg/kg per week of BNZ from weeks 50 to 55, followed by a cessation of treatment at 55 weeks and termination of the experiment at week 77 (500w/100w/STOP). The mice receiving 100 mg/kg per week of BNZ were divided in three groups on week 50 of treatment. The first group was switched to a 500 mg/kg per week of BNZ until week 77 (100w/500w). The second group continued with the same regimen of 100 mg/kg per week of BNZ until week 77 (100w/100w). In the third group, the 100 mg/kg per week treatment was stopped at week 55 (100w/STOP). In all the groups, the experiment was terminated at 77 weeks of treatment. (B) Expression of the T<sub>cm</sub> marker CD127 in blood on CD8<sup>+</sup> TSKB20-tetramer<sup>+</sup> T cells from mice untreated and undergoing different weekly treatment regimens. Data are shown as means  $\pm$  SEM. Arrows indicate the initiation of the treatment (120 dpi = week 0) and week 50, where changes in the treatment regimens occurred for the treated groups [see description in (A)]. The area in gray denotes 5 weeks corresponding to weeks 50 to 55, where the mice previously treated with BNZ at 500 mg/kg per week were switched to 100 mg/kg per week [see description in (A)]. (C) *T. cruzi* DNA isolated from skeletal muscle of untreated or treated mice at 77 weeks from experiment depicted in (A) and assayed by qPCR. A statistically significant difference was set at  $P = 0.05$ . (D) Blood from these mice collected at 77 weeks was submitted to hemoculture assays and analyzed for parasite growth for >60 days.

T cells in the blood, suggestive of reduced parasite load. By 35 weeks after treatment, the percentage of these *T. cruzi*-specific  $T_{cm}$  had plateaued in all groups (Fig. 2B), but with a clear difference between the two treated groups, with mice in the high dose group reaching average percentages of 60 to 85%  $T_{cm}$  among the *T. cruzi*-specific (TSKB20<sup>+</sup>) CD8<sup>+</sup> T cells, whereas mice in the 100 mg/kg group, on average, achieved percentages of 35 to 45%  $T_{cm}$ . Untreated mice maintained *T. cruzi*-specific  $T_{cm}$  percentages near 20% as previously reported (10, 18, 19). qPCR measurement of *T. cruzi* DNA in tissues taken at 37 weeks of treatment from a subset of animals with the highest *T. cruzi*-specific  $T_{cm}$  in the two treated groups (fig. S2, A and B) confirmed that *T. cruzi*-specific  $T_{cm}$  accurately reflected parasite load and further demonstrated that the mice from the 500 mg/kg treatment group were all parasite free by week 37 (fig. S2, C and D). Hemocultures also confirmed the persistence of infection in untreated mice and its absence in the mice treated weekly with BNZ (500 mg/kg) for 37 weeks.

These results suggested that mice in the 500 mg/kg treatment group were cured after 37 weeks of treatment but that those in the 100 mg/kg group might be a mixture of cured and not cured. To

further explore this conclusion, we modified the treatment protocol in the remaining mice at the 50-week mark, increasing or decreasing the treatment dose or stopping treatment altogether (Fig. 2A), and monitored the impact on *T. cruzi*-specific  $T_{cm}$  (Fig. 2B) and ultimately on parasite burden in tissues by qPCR (Fig. 2C). For the 500 mg/kg group, we initially lowered the weekly treatment dose to 100 mg/ml. The frequency of *T. cruzi*-specific  $T_{cm}$  remained high after this change and after stopping treatment completely at 55 weeks (Fig. 2B). When the experiment was terminated at 77 weeks after initiation of treatment (approximately 94 weeks of infection), qPCR analysis of tissues (Fig. 2C) and hemoculture of blood (Fig. 2D) from these mice confirmed the absence of infection. The mice treated at 100 mg/kg were split into three groups. In the group in which treatment was stopped at 50 weeks, the numbers of *T. cruzi*-specific  $T_{cm}$  reverted to that of mice who never received treatment and 100% of these mice had detectable parasites in tissues at 77 weeks after treatment initiation (Fig. 2, B and C). The group remaining on BNZ (100 mg/ml) maintained an intermediate frequency of *T. cruzi*-specific  $T_{cm}$  as did mice moved from 100 to 500 mg/kg treatment for >20 weeks, and both of these groups contained multiple animals with detectable parasite load at the termination of the experiment

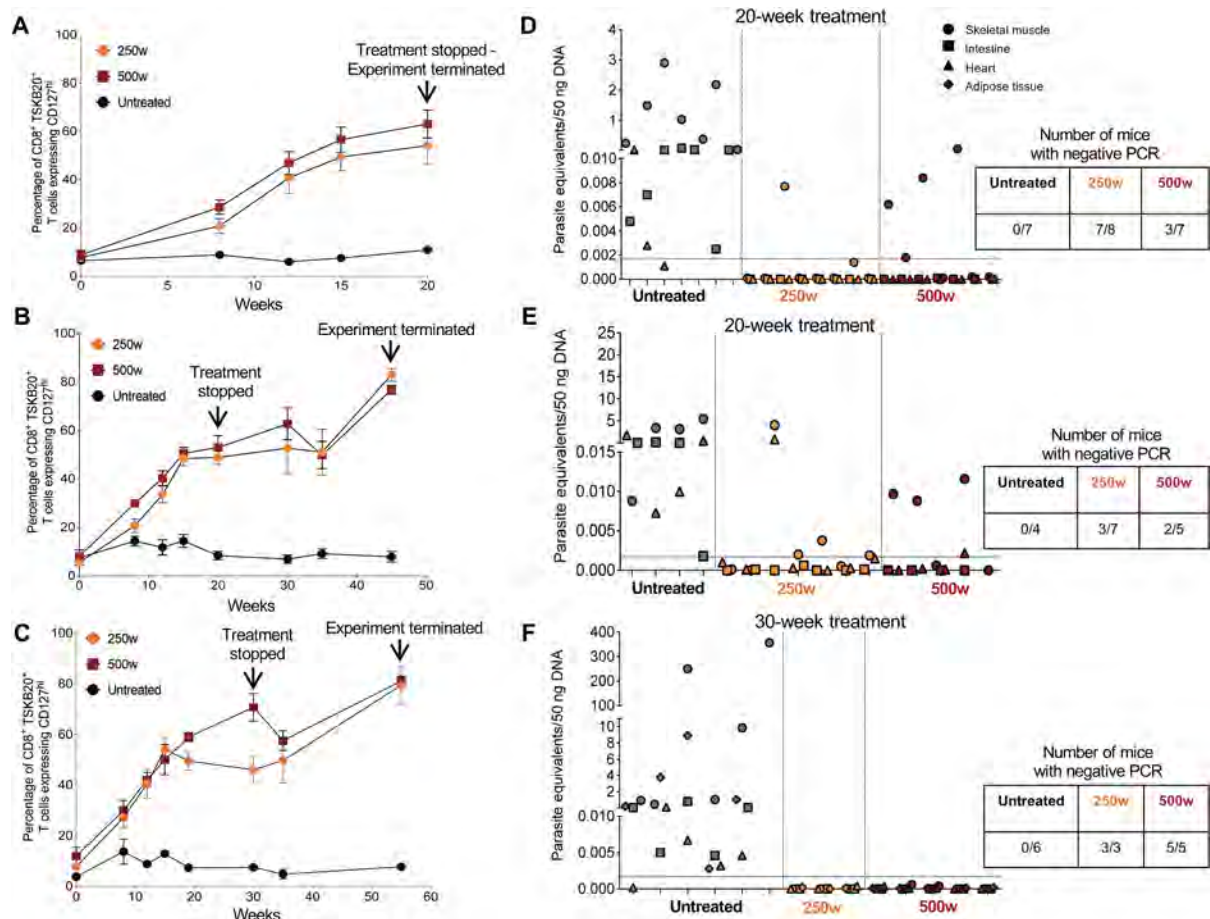


**Fig. 3. Curative effects of BNZ of weekly dosing using 2.5 to 5 times the standard daily dose in chronic *T. cruzi* infection.** C57BL/6 wild-type mice (three to eight mice in each group) were infected intraperitoneally with  $10^4$  trypomastigotes of the Colombiana strain of *T. cruzi* and left untreated or treated weekly, starting at 180 days after infection (day 0), with BNZ at a concentration of 250 or 500 mg/kg over 20 weeks (A, B, D, and E) or 30 weeks (C and F). Treatment was stopped at week 20 or 30, and assessment of treatment efficacy was carried out at week 20, 45, or 55 as indicated. (A to C) Expression of the  $T_{cm}$  marker CD127 on blood CD8<sup>+</sup> TSKB20-tetramer<sup>+</sup> T cells from mice untreated and treated with BNZ at 250 or 500 mg/kg per week. Data are shown as means  $\pm$  SEM. (D to F) Detection of *T. cruzi* DNA in samples of skeletal muscle, intestine, heart, and adipose tissue of untreated or treated mice at 20, 45, and 55 weeks and assayed by qPCR. Each x-axis hash marks tissues from an individual animal.

at week 77 (Fig. 2C). Parasites recovered from mice treated with BNZ (100 mg/kg) for 55 weeks (100w/STOP) were equally susceptible to BNZ in vitro as those isolated from untreated mice (fig. S3), indicating that the failure of this treatment regimen to resolve the infection was not due to induction of classical drug resistance. Collectively, this study showed that mice receiving a weekly dose of BNZ (500 mg/kg) for as few as 37 weeks were uniformly cured of chronic *T. cruzi* infection with a “BNZ-insensitive” strain. However, weekly treatment at the normal daily BNZ dose of 100 mg/kg failed to dependably resolve the infection, even after up to 1.5 years of treatment.

#### Weekly dosing at 2.5 to 5 times the daily dose for 30 weeks cures chronic *T. cruzi* infection

The design of the decreased frequency/extended period treatment protocol validated in the experiments above is based on the premise

that the total treatment period has to extend beyond the maximum length of amastigote dormancy to be effective. Our surrogate marker for parasitological cure—the frequency of *T. cruzi*-specific  $T_{cm}$ —plateaued at ~15 weeks of treatment with 500 mg/kg per week (Fig. 2B), establishing a potential minimal treatment period for cure. To define better the minimum treatment period needed to overcome dormancy, we initiated a weekly treatment experiment with discrete end points of 20 and 30 weeks. This experiment used a second “difficult to cure” *T. cruzi* strain, the Colombiana (10), to test the broader applicability of this dosing approach, and we included an intermediate dose group of 250 mg/kg as a dose-sparing test (Fig. 3).

Although the numbers and kinetics of *T. cruzi*-specific  $T_{cm}$  in the Colombiana infection are slightly different from that in the ARC-0704-infected mice in Fig. 2, as expected, the numbers of  $T_{cm}$  rose after initiation of the weekly BNZ treatment, reaching an

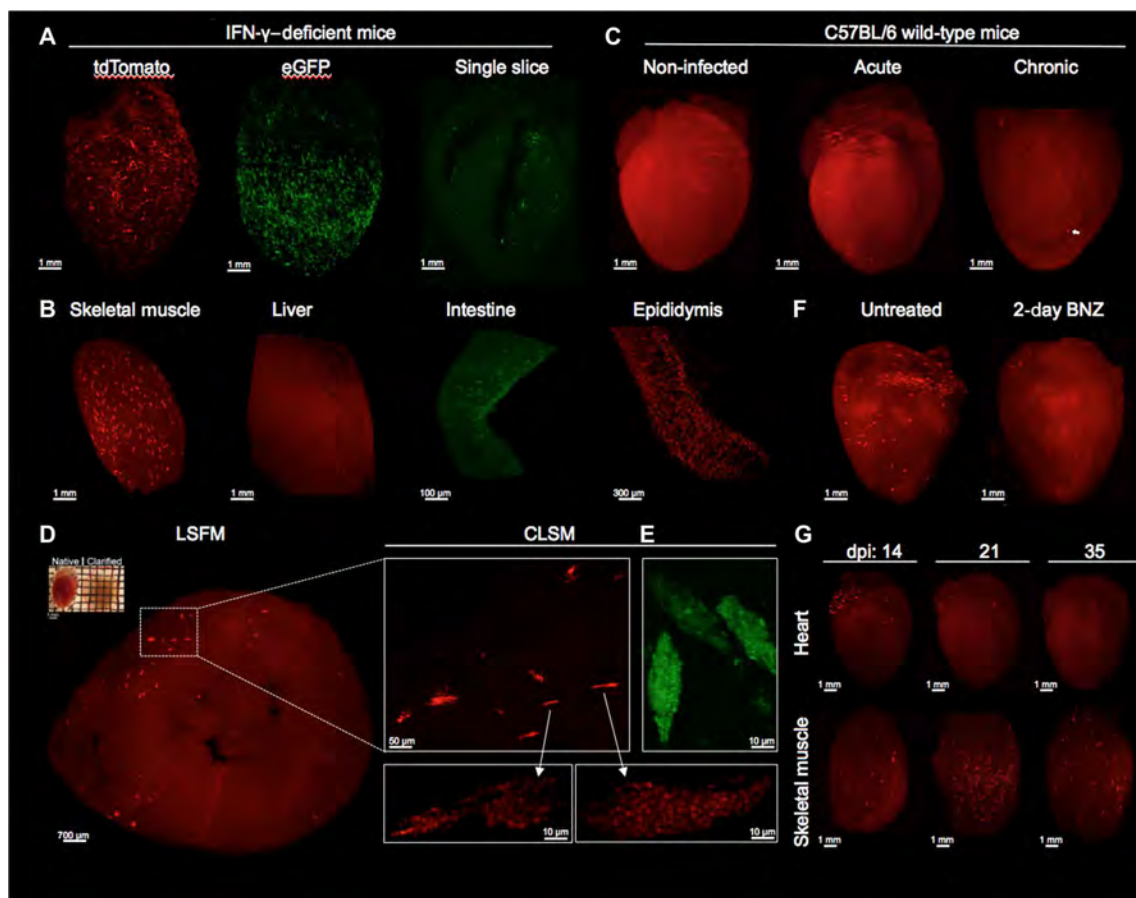


**Fig. 4. LSFM enables *T. cruzi* infection tracking in whole organs after CUBIC tissue clarification.** C57BL/6 wild-type or IFN- $\gamma$ -deficient mice were intraperitoneally infected with  $2 \times 10^5$  *T. cruzi* tdTomato-expressing Colombiana or eGFP-expressing Brazil strains. At different time points, mice were euthanized and perfused with PBS, PFA, and CUBIC clarifying cocktails. After organ collection, clarification was continued using CUBIC reagents and finally prepared for LSFM imaging. (A and B) 3D reconstruction of IFN- $\gamma$ -deficient mice organs infected with tdTomato-expressing Colombiana (red) or eGFP-expressing Brazil (green) *T. cruzi* strains in the acute phase of the infection. A single optical slice of a clarified heart shows the detection of eGFP-expressing parasites (green) throughout the organ. Amastigote nests (bright red) can be differentiated from tissue autofluorescence background (red). Low tissue autofluorescence was maintained to allow for the identification of complete organ morphology. (C) 3D reconstruction of the heart of C57BL/6 wild-type mice uninfected and infected with tdTomato-expressing Colombiana parasites in the acute and chronic phase of the infection. Arrow indicates an amastigote nest. (D) Confirmation of amastigote nests by confocal microscopy. A CUBIC-clarified heart from an acutely infected, IFN- $\gamma$ -deficient mouse (upper left) was sliced transversely in a 1-mm slice, and multiple z-stack images were obtained by LSFM. Enlarged region of interest shows nests containing tdTomato or (E) eGFP-expressing amastigotes and trypomastigotes using CLSM. (F) C57BL/6 wild-type mice infected with  $2 \times 10^5$  tdTomato-expressing Colombiana strain trypomastigotes were left untreated or treated with two daily doses (on days 18 and 19 after infection) of BNZ at a concentration of 100 mg/kg. On day 20, mice were euthanized and perfused, and the heart was clarified and prepared for LSFM. (G) C57BL/6 wild-type mice were infected with  $5 \times 10^5$  *T. cruzi* tdTomato-expressing Colombiana strain trypomastigotes. On days 14, 21, and 35 after infection, mice were euthanized, and skeletal muscle and heart were excised and clarified.

average of ~60% in all treated groups by 20 weeks of treatment (Fig. 3). However, qPCR analysis of tissues revealed that a proportion of mice in both the 250 mg or 500 mg/kg per week groups were still infected when assayed immediately after (Fig. 3, A and D) or 25 weeks after (Fig. 3, B and E) the 20-week treatment regimen. Extending the treatment to 30 weeks achieved cure in 100% of animals in both treatment groups based on qPCR (Fig. 3, C and F) and hemoculture (eight of eight samples parasite negative in treated groups and six of six samples *T. cruzi* positive in the untreated group). Thus, 30 weekly doses of BNZ (either 250 or 500 mg/kg) (2.5 to 5 times the conventional daily dose) is sufficient to obtain consistent parasitological cure in mice chronically infected with *T. cruzi* strains that are relatively resistant to cure using conventional, daily treatment regimens.

### LSFM detects *T. cruzi*-infected cells in intact tissues and organs

The above data supported our previous observations that BNZ was highly effective in rapidly killing actively dividing *T. cruzi* but apparently ineffective against dormant parasites, and the success of the extended (~30-week) treatment protocol in curing *T. cruzi* infection was consistent with an upper limit of ~30 weeks for *T. cruzi* amastigotes to remain dormant. However, direct, in vivo confirmation of these conclusions was impossible to obtain with previous approaches such as in vivo imaging, standard histology, or qPCR of tissue samples. We adopted CUBIC (clear, unobstructed brain or body imaging cocktails) tissue clarification protocols (20) and used LSFM (21, 22) technology coupled to three-dimensional (3D) organ reconstruction and automated quantification to visualize and track fluorescent protein-expressing *T. cruzi* in whole mouse organs. This approach allowed detection of *T. cruzi* not only in tissues of IFN- $\gamma$ -deficient mice (Fig. 4, A and B, and movies S1 and S2) but also in tissues of wild-type mice, including individual parasites in chronically infected tissues where parasites are very sparse (Fig. 4C and movie S3). A wide range of tissues were amenable to clarification and LSFM imaging (fig. S4). Although individual parasites could not be resolved in heavily infected cells (often referred to as “nests”) by this LSFM approach, confocal laser scanning microscopy (CLSM) of thin sections of the same clarified tissues confirmed the identification of *T. cruzi*-infected cells (Fig. 4, D and E). Supporting the results in Fig. 1, LSFM allowed us to detect the near-complete clearance of parasites in the heart following two daily doses of BNZ (Fig. 4F and movie S4). LSFM also permitted the monitoring of immune-mediated control of tissue parasite load over time in whole organs

and, for the first time, suggested a differential timing of parasite control in different tissues (Fig. 4G).

### Weekly dosing with BNZ eventually clears both actively replicating and dormant amastigotes from tissues

We next used tissue clarification coupled to LSFM to further assess the in vivo activities of BNZ ascertained from the earlier infection/treatment studies in intact tissues and organs. We infected mice with the Colombian strain of *T. cruzi* expressing tdTomato and then, starting at 5 days post-infection (dpi), treated with either 100 or 500 mg/kg per week over a period of 7 weeks. As expected, parasites became extremely rare in heart and skeletal muscle early in the treatment protocol in mice in both dosing groups, with fewer than five parasites or parasite nests per tissue (Fig. 5). However, following six to eight weekly doses, no parasites were detected in heart and skeletal muscle of mice treated with BNZ (500 mg/kg), whereas mice in the 100 mg/kg group continued to exhibit a very low, but routinely detectable number of *T. cruzi*-infected cells.

Collectively, these results confirmed the efficacy of higher-dose (500 mg/kg) weekly BNZ treatments in drastically reducing parasite load in mice and largely support the conclusions from immunological surrogates and qPCR and hemoculture-based methods of detection

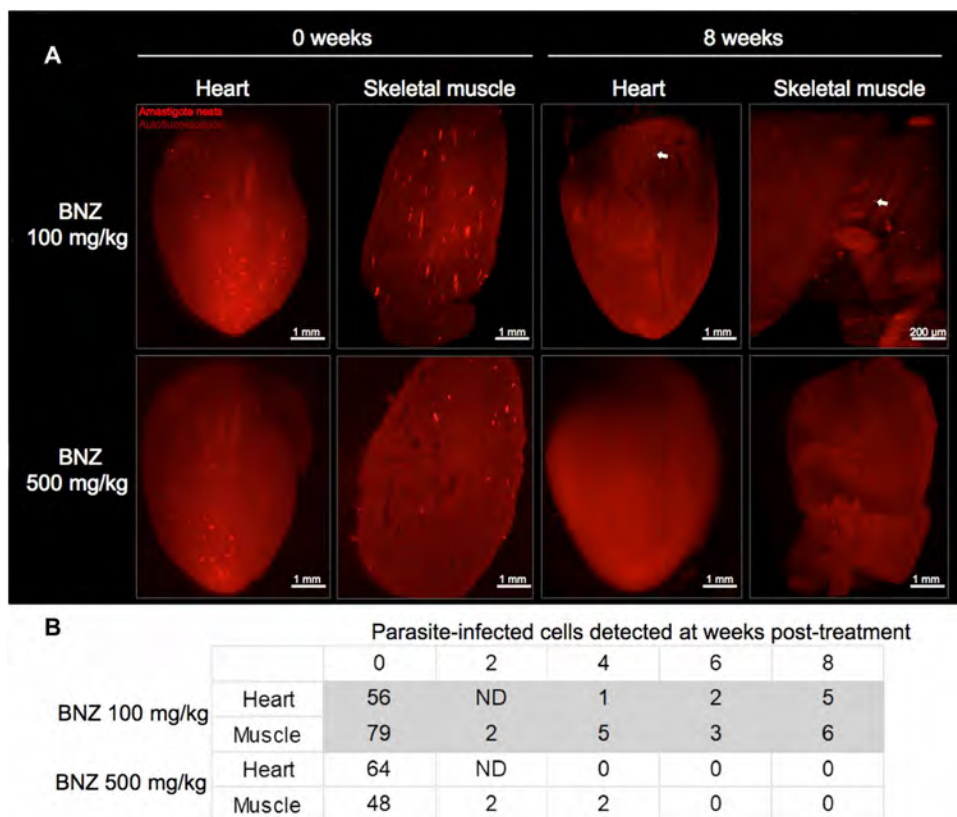


**Fig. 5. Weekly doses of BNZ (500 mg/kg) are sufficient to eliminate *T. cruzi* in heart and skeletal muscle.** C57BL/6 wild-type mice were intraperitoneally infected with  $4 \times 10^6$  tdTomato-expressing Colombian trypomastigotes of *T. cruzi* and treated weekly for 7 weeks, with BNZ (100 or 500 mg/kg), starting at 5 days after infection. At each indicated time point, one mouse per group was sacrificed and perfused, and heart and skeletal muscle were dissected, clarified, and scanned using LSFM. (A) 3D reconstructions of heart and skeletal muscle showing amastigote nests (red) in untreated (0 weeks) and treated (8 weeks) mice. Arrows indicate amastigote nests. (B) Automated quantification of total *T. cruzi* amastigote nests in tissue 3D reconstructions. ND, not determined.

of parasite persistence as shown in Figs. 1 and 2. These results also suggested that the higher dose weekly treatment regimen was eventually clearing dormant parasites, whereas the lower dose treatment was not. To directly address this point, we infected mice with the tdTomato-expressing and DiR near-infrared cyanine dye-stained trypomastigotes of the Colombiana strain of *T. cruzi*. The use of the DiR fluorescent dye allows us to track dormant parasites by visualizing those that had not diluted the dye as a result of replication [as shown for CellTrace Violet in our previous studies (9)]. We first confirmed that DiR fluorescence survived the CUBIC clearing process (fig. S7). Unexpectedly, mice treated weekly at 500 mg/kg BNZ showed loss of both replicating and nonreplicating (dormant) amastigotes in heart, skeletal muscle, and intestine within 6 weeks (Fig. 6, A to C; movie S5; and table S1), whereas mice receiving the 100 mg/kg dosage over 11 weeks had persistent actively dividing and dormant parasites in these tissues (table S2).

## DISCUSSION

Chagas disease is a progressive disease caused by persistent infection with *T. cruzi*, and prevention of this disease almost certainly requires sterile parasitological cure; simply reducing parasite burden does not prevent disease progression. For this reason, the recent identification of dormancy in *T. cruzi* amastigotes is particularly concerning, as there is a dearth of information on the mechanism of this process, and current drugs appear to have modest, if any, effect on the dormant stages. A number of long-used (BNZ and NFX) and other initially promising new candidates with potent *in vitro* anti-*T. cruzi* activity (23–27) routinely fail to cure infection, and this failure is, at least in part, due to the lack of impact of these compounds on dormant forms.

The recognition of dormancy as a factor in treatment failure also provides a path for improving treatment efficacy by specifically targeting dormant forms. In this study, we identified a treatment protocol that uses a readily available, U.S. Food and Drug Administration–approved compound in a rationally designed regimen that consistently provided sterile parasitological cure. This outcome was achieved under the most rigorous infection conditions using difficult to cure parasite strains and established, chronic infections and was validated using previously authenticated immunological and parasitological protocols and, further, with a newly

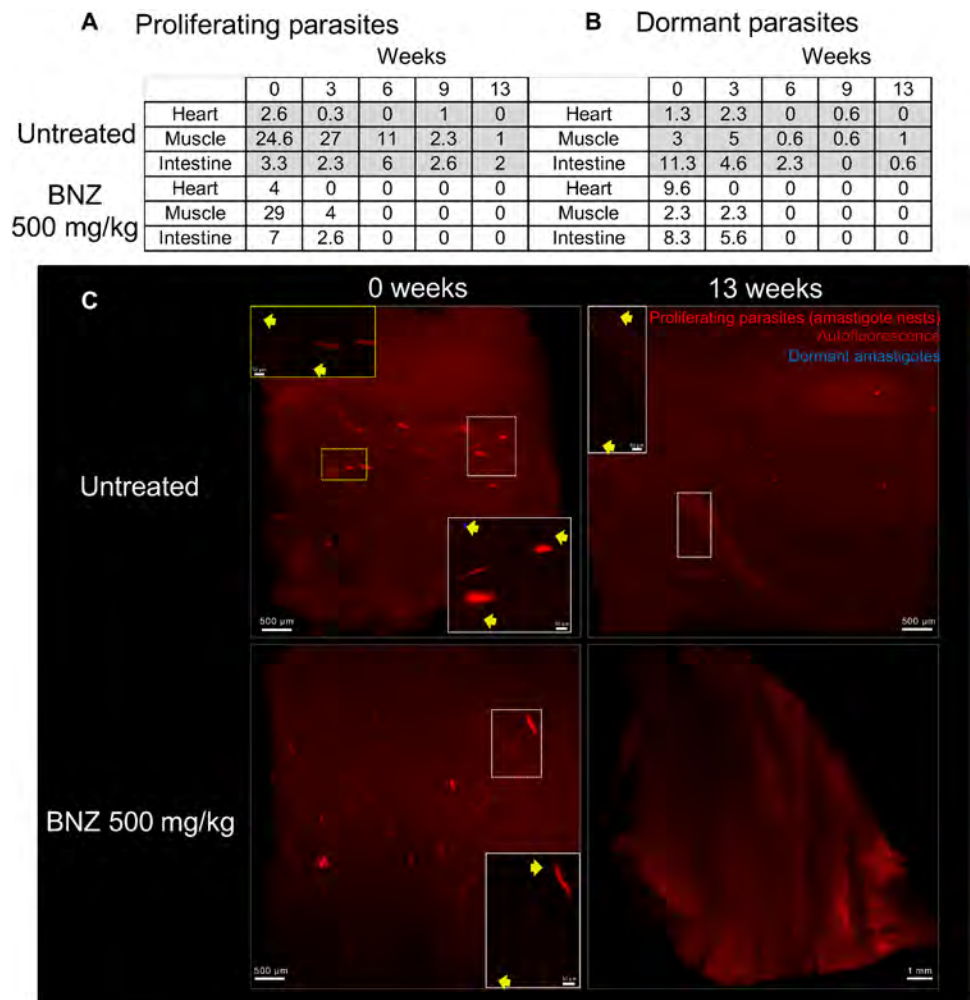


**Fig. 6. Active and dormant parasites decline after weekly treatment with BNZ (500 mg/kg).** C57BL/6 wild-type mice (15 mice per group) were intraperitoneally infected with  $4 \times 10^6$  trypomastigotes of the tdTomato-expressing Colombiana strain of *T. cruzi* stained with DiR near-infrared dye. Mice were untreated or treated weekly, starting 37 days after infection, with BNZ at a concentration of 500 mg/kg over 12 weeks. On weeks 0, 3, 6, 9, and 13, three mice per group were euthanized and perfused. After dissection of the heart, muscle and intestine tissues were clarified and scanned by LSFM. **(A)** Automated quantification of total tdTomato-positive parasite nests in 3D reconstructions of the heart, skeletal muscle, and intestine of mice untreated and treated with BNZ (500 mg/kg). The results correspond to the average number of nests in tissue samples from three individual mice (table S1A). **(B)** Automated quantification of total DiR-positive dormant parasites. The results correspond to the average number of dormant parasites in tissue samples from three individual mice (table S1B). **(C)** Representative 3D reconstructions of skeletal muscle showing tdTomato-positive parasite nests (red) and DiR-positive dormant individual amastigotes (blue) in untreated (0 weeks) and treated (13 weeks) mice. Yellow arrows indicate DiR-positive dormant amastigotes.

established tissue clearing/LSFM approach that allows detection of host cells containing individual, including dormant, amastigotes in whole organs.

The high-dose, extended-time protocol evaluated in this study considered characteristics of *T. cruzi* infection that were not appreciated when the standard daily administration protocol was developed nearly 50 years ago, and its success depended on both extending the BNZ treatment period (to 30 weeks) and increasing each dose to at least 2.5 times what is normally used in daily dosing regimens. The extended treatment period may be necessary to challenge the stochastic nature of dormancy in *T. cruzi* (9, 10). The successful cure using a 30-week (but not 20-week) treatment regimen in chronically

infected mice indicates that the ability of amastigotes to remain quiescent is time limited.

The absolute requirement for a higher dose of BNZ in this protocol became evident from the rapid rebound in parasite growth after a single standard (100 mg/kg) dose of BNZ (Fig. 1) and was confirmed by the evidence of persisting parasites in tissues by LSFM and by qPCR in mice treated for as long as 1 year at this dose. In contrast, mice receiving 2.5 to 5 times the standard BNZ dose showed clearance of both actively dividing and (eventually) nondividing amastigotes, establishing that insufficient dosing for BNZ is a second factor in the frequent failure of current protocols, which needs to be reconsidered in all species.

The two variables of BNZ dose and length of treatment have not previously been thoroughly evaluated in concert in *T. cruzi* infection. However, because the higher BNZ dosage has a sustained impact on actively replicating *T. cruzi* [despite a half-life of ~12 hours in mice (28, 29)], it is possible to both increase the dose of BNZ and extend the length of treatment using approximately one-third the weekly dose of standard protocols while only marginally increasing total cumulative exposure over the 30-week treatment period, relative to the conventional 60-day, daily treatment course.

A limitation of our study is that the dosing regimen was evaluated only in mice. However, mice have proven to be extremely reliable indicators of drug efficacy (and other aspects) in Chagas disease, when appropriately used and carefully evaluated (9, 10, 18, 30). The length of treatment is also a disadvantage of this new protocol as is the higher bolus with each treatment, which could increase the potential for toxicity, although we observed no toxicity of these regimens in mice. Additional modifications, such as twice-weekly dosing, not only might shorten the treatment period but also risk increasing side effects. Ongoing studies in dogs and nonhuman primates should be informative on these points.

An unexpected finding using LSFM to monitor the attrition of dye-positive dormant amastigotes over time is that these dormant amastigotes declined more rapidly in mice under weekly BNZ treatment than in untreated mice. This is counter to our interpretation of previous studies (9) and suggests that dormant parasites are not totally refractory to BNZ treatment, particularly at the higher doses used in this protocol, an encouraging hint that dormant *T. cruzi* are accessible to some compounds. Furthermore, the very rapid and highly efficient clearance of actively replicating *T. cruzi* with one dose of BNZ suggests that, if combined with a compound that rapidly reverses *T. cruzi* dormancy, a completely curative treatment requiring only a few days of treatment—perhaps even with a single combined dose—could be developed.

Last, this study introduces new protocols to quantify both actively dividing and individual dormant parasites in intact tissues and organs. Assessment of parasite numbers using LSFM of clarified tissues should be integrated into protocols for comparison of therapeutic regimens, and assessment of new candidate drugs and variations on this basic technique will be useful in understanding parasite behavior in vivo, immune responses to parasites, and generation of tissue damage—issues that have previously been approached only via highly selective sampling of tissue slices via histology—in whole organs. Collectively, the imaging of *T. cruzi* in clarified tissues also affords new appreciation of the morphology of infected cells, the variability in distribution of infected cells within tissues, and the heavy bias for infection of muscle cells in the various tissues and provides a method to study strain variability, drug sensitivity, tissue

distribution, and immune response in this and other host-pathogen interactions.

## MATERIALS AND METHODS

### Study design

In this study, we have developed and evaluated a long-term but less-intensive drug-sparing BNZ treatment protocol that provides 100% cure rates in mice chronically infected with *T. cruzi*. The determination of treatment efficacy was assessed by flow cytometry, qPCR, hemocultures, and whole-body luciferase imaging. In addition, we established tissue clearing and LSFM methods that allow the quantification of actively replicating and dormant parasites in whole tissues/organs. Details regarding these techniques are available below. Female and male mice, 8 to 12 weeks old, were used for infections throughout the study. The sample size and infection dose are provided in each figure legend. Sample size was determined based on our knowledge of heterogeneity in parasite burden during *T. cruzi* infection and published reports using similar experimental strategies. Data collected were included if productive *T. cruzi* infection was established (visualized by luciferase imaging or flow cytometry by detection of *T. cruzi* tetramer-specific CD8<sup>+</sup> T cells). The investigators were not blinded during the collection or analysis of data, and mice were randomly assigned to treatment groups before the start of each experiment.

### Mice, parasites, and infections

C57BL/6J (stock no. 000664) mice (C57BL/6 wild type) were purchased from The Jackson Laboratory (Bar Harbor, ME), and C57BL/6J-IFN- $\gamma$  knockout mice (also known as B6.129S7-Ifngtm1Ts/J; The Jackson Laboratory, stock no. 002287) (IFN- $\gamma$  deficient) were bred in-house at the University of Georgia Animal Facility. All the animals were maintained in the University of Georgia Animal Facility under specific pathogen-free conditions. *T. cruzi* tissue culture trypomastigotes of the wild-type strains Brazil, Colombiana, and ARC-0704 were maintained through passage in Vero cells (American Type Culture Collection, Manassas, VA) cultured in RPMI 1640 medium with 10% fetal bovine serum (FBS) at 37°C in an atmosphere of 5% CO<sub>2</sub>. Also, in this study, we use the Brazil strain expressing enhanced green fluorescent protein (eGFP) and the Colombiana strain coexpressing firefly luciferase and tdTomato reporter proteins generated as described previously (9, 31). Mice were infected subcutaneously in the footpad, intraperitoneally or intramuscularly with tissue culture trypomastigotes of *T. cruzi*, and euthanized by carbon dioxide inhalation. This study was carried out in strict accordance with the Public Health Service Policy on Humane Care and Use of Laboratory Animals and Association for Assessment and Accreditation of Laboratory Animal Care accreditation guidelines. The protocol was approved by the University of Georgia Institutional Animal Care and Use Committee.

### Drug treatment and in vivo imaging

Infected mice were treated according to the indicated schedules. BNZ (Elea Phoenix) was prepared by pulverization of tablets followed by suspension in an aqueous solution of 1% sodium carboxymethylcellulose with 0.1% Tween 80 and delivered orally by gavage at a concentration dosage of 100, 250, or 500 mg/kg body weight. Each mouse received 0.2 ml of this suspension. Luciferase-expressing parasites were quantified in mice by bioluminescent detection. Mice were injected

intraperitoneally with D-luciferin (150 mg/kg; PerkinElmer) and anesthetized using 2.5% (v/v) gaseous isoflurane in oxygen before imaging on an IVIS Lumina II imager (Xenogen) as previously described (30). Quantification of bioluminescence and data analysis was performed using Living Image v4.3 software (Xenogen). Exposure time was 5 min.

### T cell phenotyping

Mouse peripheral blood was obtained by retro-orbital venipuncture and collected in sodium citrate solution, red blood cells were lysed, and the remaining cells were washed in staining buffer [2% bovine serum albumin, 0.02% azide in phosphate-buffered saline (PBS) (PAB)] as previously described (10). Whole blood was incubated with a major histocompatibility complex I (MHC I) tetramer containing the specific TSKB20 peptide (ANYKFTLV/Kb) labeled with BV421 (Tetramer Core Facility at Emory University, Atlanta, GA) and the following labeled antibodies: anti-CD8 fluorescein isothiocyanate (FITC), anti-CD4 allophycocyanin (APC) EF780, and anti-CD127 phycoerythrin (PE) (BD Biosciences). For whole blood, we lysed red blood cells in a hypotonic ammonium chloride solution after washing twice in PAB. We stained cells for 45 min at 4°C in the dark, washed them twice in PAB, and fixed them in 2% formaldehyde. At least 500,000 cells were acquired using a CyAn ADP flow cytometer (Beckman Coulter) and analyzed with FlowJo software v10.6.1 (Treestar Inc.).

### In vitro maximal luminescence ATP detection assay

*T. cruzi* epimastigotes from the ARC-0704 strain were used in this assay. Parasites were isolated from tissue culture or hemocultures at 77 weeks from mice untreated or treated with BNZ (100 mg/kg) and submitted to termination of the treatment at week 55. Approximately 25,000 log-phased epimastigotes were subjected to serial twofold dilutions of BNZ starting at 80 μM for 4 days before measuring their adenosine triphosphate (ATP) production using ATPlite Luminescence ATP Detection Assay System (PerkinElmer). Luminescence was read using a BioTek Synergy Hybrid Multi-Mode reader (BioTek). A dose-response curve was generated with GraphPad Prism 5.0 (GraphPad Software Inc.). IC<sub>50</sub> was determined as the drug concentration that was required to inhibit 50% of ATP production compared to that of parasites with no drug exposure.

### qPCR and hemoculture

Mouse tissue samples of skeletal muscle, heart, intestine, and adipose tissue were collected at various time points and processed for quantification of *T. cruzi* DNA by real-time qPCR. DNA from mouse tissues was extracted using the protocol included with the Qiagen DNeasy Blood and Tissue Kit (Qiagen). Following the spin-column protocol for "Purification of Total DNA from Animal Tissues," approximately 100-μl piece of tissue from the desired animal was minced finely using microdissecting scissors (MilliporeSigma) and proceeded with the extraction protocol as described by the manufacturer. All DNA samples were diluted to 25 ng/μl in nuclease-free water. The generation of PCR standards and detection of parasite tissue load by qPCR was carried out as previously described (10, 18, 32). For the qPCRs, we used the *T. cruzi* primers S35 (AAATAATGTACGGGKAGATGCATGA) and S36 (GGGTTGGATTGGG-GTTGGTGT) as well as tumor necrosis factor (TNF) housekeeping gene primers 5411 (CAGCAAGCATCTATGCACTTAGACCCC) and 5241 (TCCCTCTCATCAGRRCTATGGCCCA). qPCRs con-

sisted of 50 ng of genomic DNA: 0.5 μM of each primer set along with 10 μl of IQ SYBR Green and water to make a 20-μl final volume reaction. C1000 Touch Bio-Rad CFX96 real-time PCR detection system was used under the following cycling conditions: (i) initial denaturation, 95°C, 10 min; (ii) denaturation, 95°C, 15 s; (iii) annealing, 60°C, 15 s; (iv) extension, 72°C, 15 s; (v) plate read; (vi) ×40 cycles; (vii) 95°C, 1 s; (viii) melt curve creation, 60° to 93°C, 30 s, 0.5°C per cycle; lid 105°C. The range of standards for these particular assays was  $1.7 \times 10^2$  to  $1.7 \times 10^{-3}$ . For each tissue type, a TNF reference was included matching that tissue type. A twofold serial dilution was used to create eight standards for TNF comparison. Analysis of the data was done using CFX Manager software version 3.1 (Bio-Rad). Samples were analyzed by looking at the starting quantity (SQ) mean value for each replicate and making an average of two replicates per mouse sample for both S35/36 and TNF primer reactions. S35/36 SQ mean values were compared to the S35/36 standard curve, whereas the TNF SQ mean values were compared to the TNF standard curve for each respective plate. The S35/36 average SQ mean value was then divided by the TNF average SQ mean value and multiplied by 50 to reach the parasite equivalence per 50 ng of DNA. The limit of detection was set at the lowest standard 0.0017. For hemoculture determinations, peripheral blood from infected mice was collected and cultured at 26°C in supplemented liver digest neutralized tryptose medium as described previously (33). The presence of *T. cruzi* parasites was assessed every week for 3 months under an inverted microscope.

### Tissue clearing

Multiple tissue clearing protocols were tested (SCALE, CLARITY, uDISCO, iDISCO, vDISCO, and FDISCO); however, tdTomato or eGFP parasite fluorescence was best preserved using CUBIC. All the tissue clearings performed in this work were done using CUBIC protocol I (20). We use three different cocktails: CUBIC-P for delipidation and rapid decolorization: 5 weight % (wt %) 1-methylimidazole, 10 wt % *N*-butyldiethanolamine, and 5 wt % Triton X-100; CUBIC-L for delipidation and decolorization: 10 wt % *N*-butyldiethanolamine and 10 wt % Triton X-100; and CUBIC-R for refractive index (RI) matching: 10 wt % 1,3-bis(aminomethyl)cyclohexane, 10 wt % sodium dodecylbenzenesulfonate, pH 12.0 adjusted by *p*-toluenesulfonic acid. Mice (C57BL/6 wild type and IFN-γ deficient) were euthanized by carbon dioxide inhalation. As soon as the animals did not show any pedal reflex, they were intracardially perfused with 50 ml of PBS (pH 7.4): 50 ml of 4% (w/v) paraformaldehyde (PFA) in PBS and 100 ml of CUBIC-P cocktail. After perfusions, the organs were dissected and immersed individually in 10 ml of 1:1 water-diluted CUBIC-L using 50-ml falcon tubes (Thermo Fisher Scientific) in an orbital shaker (150 rpm) at 37°C overnight. The next day, tissues were immersed in 10 ml of 100% CUBIC-L for 6 days (refreshing the solution on day 3) and washed with 30 ml of 1× PBS overnight shaking at room temperature. To avoid tissue damage, organs were maintained in the same tube during the complete protocol and solutions were collected using a vacuum system. The organs were then immersed in 1:1 water-diluted CUBIC-R solution with shaking (150 rpm) at room temperature overnight and then immersed in 100% CUBIC-R with shaking (150 rpm) at room temperature for 2 to 3 days. To eliminate bubbles inside the heart and/or tissue surfaces, CUBIC-R solution was carefully dried out using cleaning wipes (Kimwipes, Kimberly-Clark) and then incubated in 10 ml of immersion oil (RI = 1.51, Cargille Laboratories) using six-well

cell culture plates (Thermo Fisher Scientific). The next day, remaining bubbles were discarded by using tweezers. Organs were adhering to a flat-top sample holder (LaVision BioTec) by using cyanoacrylate-based gel superglue (Scotch). Whole organs were imaged transversally to their longitudinal axis. Hearts were glued with the apex and the aorta horizontally aligned. For image acquisition, cleared samples were immersed in 100 to 120 ml of immersion oil in a quartz cuvette and prepared for LSMF imaging.

### LSFM and image processing

CUBIC transparent organs were imaged in 3D using an Ultramicroscope II imaging system and Inspector software (both from LaVision BioTec). This light sheet microscope was equipped with an Olympus MVX10 Zoom Body (Olympus); a LaVision BioTec Laser Module with 488-, 561-, 640-, and 785-nm laser lines; and an Andor Neo sCMOS camera with a pixel size of 6.5  $\mu\text{m} \times 6.5 \mu\text{m}$ . Organs were imaged at 1.26 $\times$  using right and left light sheet (three on each side) lasers with 5  $\mu\text{m}$  thickness and 100% width. The exposure time was kept constant at 50 ms, and the laser power was adjusted from 10 to 80% depending on the intensity of the fluorescence signal. Step size between individual slices was adjusted to 3  $\mu\text{m}$ . A variable number of TIFF images were obtained depending on organ size ranging from 300 to 1500. TIFF stacks were converted (ImarisFileConverterx64, v9.2.0, Bitplane AG) into Imaris files (.ims). 3D reconstruction and subsequent analysis was done using Imaris software v9.3 (Bitplane AG). Movies were generated by Imaris using a total of 800 frames reproduced at 24 frames per second (fps). 2D slice animations were generated by the orthoslicer Imaris software tool and reproduced at 24 fps. Movies were edited and transcoded by the open-source software OpenShot v2.5.1 (OpenShot Studios) and HandBrake v1.3.1 (The HandBrake Team), respectively. Supplementary movies were strongly downsampled to accommodate the large original datasets. The loss of optical image quality in the movies was kept at a minimum; however, it was impossible to avoid completely.

### Automated parasite quantification

For the quantification of parasite nests and dormant parasites, appropriate threshold of signals from reporter proteins was selected in each experiment. Automatic cell counting tool under the spot detection algorithm was performed using Imaris software. An initial analysis was performed in a randomly selected 3D region of interest (ROI) and then applied to the entire 3D organ reconstruction. For the automated counting of amastigote nests, we selected the 532-nm channel and then counted elongated forms with up to 200- $\mu\text{m}$  radius distance. To identify DiR near-infrared positive dormant parasites, we selected the 639-nm channel to count cells of 3- to 5- $\mu\text{m}$  radius distance. Artifacts within tissues are usually bright in multiple channels. We take advantage of this property to discard artifacts by imaging using an additional channel (often 488-nm channel). Double-color objects (GFP/tdTomato or GFP/DiR near infrared) were considered artifacts and not considered for counting.

### CLSM imaging

Confocal fluorescence imaging was performed using a Zeiss LSM 710 inverted confocal microscope attached to an EXFO Xcite series 120Q lamp and a digital Zeiss XM10 camera (Carl Zeiss AG). For LSMF validation experiments, a transparent section of the heart was placed on a 35-mm glass-bottom petri dish and mounted in a drop of immersion oil before imaging using  $\times 10$  and  $\times 100$  objectives.

The peritoneal adipose tissue was placed over a surface of  $\sim 1.6 \text{ cm}^2$ , and the skeletal muscle was sliced into thin sections and mounted using ProLong Diamond antifade solution (Thermo Fisher Scientific). Tissue slices were exhaustively scanned, and the images were taken using  $\times 63$  objectives. Zeiss Zen software was used to process the optical z-stack sections into a single 2D image.

### Labeling of parasites with fluorescent dyes

Cell suspensions of *T. cruzi* trypomastigotes were labeled with the near-infrared fluorescent cyanine dye DiR [DiIC<sub>18</sub>(7);1,1'-diiododecyl-3,3,3',3'-tetramethylindotricarbocyanine iodide] (Biotium) following the manufacturer's instructions. Briefly,  $1 \times 10^6$  trypomastigotes were incubated for 20 min at 37°C with DiR (2  $\mu\text{g}/\text{ml}$ ), protected from light. Unbound dye was quenched by the addition of five volumes of  $1 \times \text{PBS}$ . After an additional washing in warm FBS-RPMI, parasites were used for infection of cell cultures or mice. For DiR and CellTrace Far Red costaining,  $1 \times 10^6$  trypomastigotes were incubated for 20 min at 37°C with DiR (2  $\mu\text{g}/\text{ml}$ ) and 10  $\mu\text{M}$  CellTrace Far Red (CellTrace Cell Far Red Proliferation Kit, Thermo Fisher Scientific), protected from light. The quenching of unbound dyes was performed as previously described.

### Statistical analysis

The Mann-Whitney *U* tests and one-way analysis of variance (ANOVA) of the GraphPad Prism version 5.0 software were used. Values are expressed as means  $\pm$  SEM of at least three separate experiments. *P* values equal to or less than 0.05 were considered significant.

### SUPPLEMENTARY MATERIALS

stm.sciencemag.org/cgi/content/full/12/567/eabb7656/DC1

Fig. S1. Tissue persistence of ARC-0704 *T. cruzi* strain pre- and post-full course BNZ treatment in chronically infected mice.

Fig. S2. BNZ given weekly over 37 weeks cures mice with chronic *T. cruzi* infections.

Fig. S3. Parasites recovered from mice treated for 55 weeks with 100 mg/kg of BNZ (100w/STOP) had unchanged susceptibility to BNZ in vitro.

Fig. S4. 3D reconstruction of whole organs from uninfected C57BL/6 mice.

Fig. S5. *T. cruzi* clearance as assessed by whole-organ LSMF.

Fig. S6. Drug dose-dependent differential clearance of an established *T. cruzi* infection as assessed by confocal microscopy.

Fig. S7. CUBIC tissue clarification protocols preserve fluorescence in dye-stained parasites.

Table S1. Automated quantification of total tdTomato-positive amastigote nests or total DiR-positive dormant parasites in tissues of untreated and treated mice with 500 mg/kg of BNZ.

Table S2. Automated quantification of total DiR-positive dormant parasites from the experiment performed in Fig. 5 and Fig. S5.

Movie S1. Nearly unrestricted expansion of *T. cruzi* amastigote nests in heart and skeletal muscle in IFN- $\gamma$ -deficient mice.

Movie S2. Uncontrolled *T. cruzi* development in IFN- $\gamma$ -deficient mice.

Movie S3. Controlled *T. cruzi* amastigote nests in infected C57BL/6 wild-type mice.

Movie S4. Partial clearance of *T. cruzi* parasites following brief BNZ treatment.

Movie S5. Multicolor light sheet microscopy reveals active and dormant parasite clearance following weekly BNZ treatment.

Raw data file. Raw data file.xlsx.

[View/request a protocol for this paper from Bio-protocol.](#)

### REFERENCES AND NOTES

- C. J. Schoffeld, J. Jannin, R. Salvatella, The future of Chagas disease control. *Trends Parasitol.* **22**, 583–588 (2006).
- P. J. Hotez, D. H. Molyneux, A. Fenwick, J. Kumaresan, S. E. Sachs, J. D. Sachs, L. Savioli, Control of neglected tropical diseases. *N. Engl. J. Med.* **357**, 1018–1027 (2007).
- WHO, Chagas disease in Latin America: An epidemiological update based on 2010 estimates. *Wkly. Epidemiol. Rec.* **90**, 33–44 (2015).
- J. Rodrigues Coura, S. L. de Castro, A critical review on Chagas disease chemotherapy. *Mem. Inst. Oswaldo Cruz* **97**, 3–24 (2002).

5. J. A. Urbina, Specific chemotherapy of Chagas disease: Relevance, current limitations and new approaches. *Acta Trop.* **115**, 55–68 (2010).
6. R. Viotti, C. Vigliano, B. Lococo, M. G. Alvarez, M. Petti, G. Bertocchi, A. Armenti, Side effects of benznidazole as treatment in chronic Chagas disease: Fears and realities. *Expert Rev. Anti Infect. Ther.* **7**, 157–163 (2014).
7. M. G. Álvarez, Y. Hernández, G. Bertocchi, M. Fernández, B. Lococo, J. C. Ramirez, C. Cura, C. L. Albizu, A. Schijman, M. Abril, S. Sosa-Estani, R. Viotti, New scheme of intermittent benznidazole administration in patients chronically infected with *Trypanosoma cruzi*: A pilot short-term follow-up study with adult patients. *Antimicrob. Agents Chemother.* **60**, 833–837 (2016).
8. J. Alonso-Padilla, N. Cortés-Serra, M. J. Pinazo, M. E. Bottazzi, M. Abril, F. Barreira, S. Sosa-Estani, P. J. Hotez, J. Gascón, Strategies to enhance access to diagnosis and treatment for Chagas disease patients in Latin America. *Expert Rev. Anti Infect. Ther.* **17**, 145–157 (2019).
9. F. J. Sánchez-Valdez, A. Padilla, W. Wang, D. Orr, R. L. Tarleton, Spontaneous dormancy protects *Trypanosoma cruzi* during extended drug exposure. *eLife* **7**, e34039 (2018).
10. J. M. Bustamante, J. M. Craft, B. D. Crowe, S. A. Ketchie, R. L. Tarleton, New, combined, and reduced dosing treatment protocols cure *Trypanosoma cruzi* infection in mice. *J. Infect. Dis.* **209**, 150–162 (2013).
11. M. P. Barrett, D. E. Kyle, L. D. Sibley, J. B. Radke, R. L. Tarleton, Protozoan persister-like cells and drug treatment failure. *Nat. Rev. Microbiol.* **17**, 607–620 (2019).
12. E. Aldasoro, E. Posada, A. Requena-Méndez, A. Calvo-Cano, N. Serret, A. Casellas, S. Sanz, D. Soy, M. J. Pinazo, J. Gascon, What to expect and when: Benznidazole toxicity in chronic Chagas' disease treatment. *J. Antimicrob. Chemother.* **73**, 1060–1067 (2018).
13. J. A. Castro, M. M. de Mecca, L. C. Bartel, Toxic side effects of drugs used to treat Chagas' disease (American trypanosomiasis). *Hum. Exp. Toxicol.* **25**, 471–479 (2006).
14. C. R. F. Marinho, L. N. Nuñez-Apaza, R. Martins-Santos, K. R. B. Bastos, A. L. Bombeiro, D. Z. Bucci, L. R. Sardinha, M. R. D. Lima, J. M. Alvarez, IFN- $\gamma$ , but not nitric oxide or specific IgG, is essential for the *in vivo* control of low-virulence Sylvio X10/4 *Trypanosoma cruzi* parasites. *Scand. J. Immunol.* **66**, 297–308 (2007).
15. M. L. Ferraz, R. T. Gazzinelli, R. O. Alves, J. A. Urbina, A. J. Romanha, The Anti-*Trypanosoma cruzi* activity of posaconazole in a murine model of acute Chagas' disease is less dependent on gamma interferon than that of benznidazole. *Antimicrob. Agents Chemother.* **51**, 1359–1364 (2007).
16. S. G. Andrade, J. B. Magalhaes, A. L. Pontes, Evaluation of chemotherapy with benznidazole and nifurtimox in mice infected with *Trypanosoma cruzi* strains of different types. *Bull. World Health Organ.* **63**, 721–726 (1985).
17. H. R. Martins, L. M. Figueiredo, J. C. O. Valamiel-Silva, C. M. Carneiro, G. L. L. Machado-Coelho, D. M. Vitelli-Avelar, M. T. Bahia, O. A. Martins-Filho, A. M. Macedo, M. Lana, Persistence of PCR-positive tissue in benznidazole-treated mice with negative blood parasitological and serological tests in dual infections with *Trypanosoma cruzi* stocks from different genotypes. *J. Antimicrob. Chemother.* **61**, 1319–1327 (2008).
18. J. M. Bustamante, L. M. Bixby, R. L. Tarleton, Drug-induced cure drives conversion to a stable and protective CD8<sup>+</sup> T central memory response in chronic Chagas disease. *Nat. Med.* **14**, 542–550 (2008).
19. L. M. Bixby, R. L. Tarleton, Stable CD8<sup>+</sup> T cell memory during persistent *Trypanosoma cruzi* infection. *J. Immunol.* **181**, 2644–2650 (2008).
20. K. Tainaka, T. C. Murakami, E. A. Susaki, C. Shimizu, R. Saito, K. Takahashi, A. Hayashi-Takagi, H. Sekiya, Y. Arima, S. Nojima, M. Ikemura, T. Ushiku, Y. Shimizu, M. Murakami, K. F. Tanaka, M. Iino, H. Kasai, T. Sasaoka, K. Kobayashi, K. Miyazono, E. Morii, T. Isa, M. Fukayama, A. Kakita, H. R. Ueda, Chemical landscape for tissue clearing based on hydrophilic reagents. *Cell Rep.* **24**, 2196–2210.e9 (2018).
21. F. Pampaloni, B.-J. Chang, E. H. K. Stelzer, Light sheet-based fluorescence microscopy (LSFM) for the quantitative imaging of cells and tissues. *Cell Tissue Res.* **360**, 129–141 (2015).
22. J. Swoger, F. Pampaloni, E. H. K. Stelzer, Light-sheet-based fluorescence microscopy for three-dimensional imaging of biological samples. *Cold Spring Harb. Protoc.* **2014**, 1–8 (2014).
23. A. F. Francisco, M. D. Lewis, S. Jayawardhana, M. C. Taylor, E. Chatelain, J. M. Kelly, Limited ability of posaconazole to cure both acute and chronic *Trypanosoma cruzi* infections revealed by highly sensitive *in vivo* imaging. *Antimicrob. Agents Chemother.* **59**, 4653–4661 (2015).
24. F. Torrico, J. Gascon, L. Ortiz, C. Alonso-Vega, M. J. Pinazo, A. Schijman, I. C. Almeida, F. Alves, N. Strub-Wourgaft, I. Ribeiro; E1224 Study Group, Treatment of adult chronic indeterminate Chagas disease with benznidazole and three E1224 dosing regimens: A proof-of-concept, randomised, placebo-controlled trial. *Lancet Infect. Dis.* **18**, 419–430 (2018).
25. T. A. F. Martins, L. de Figueiredo Diniz, A. L. Mazzeti, A. F. da Silva do Nascimento, S. Caldas, I. S. Caldas, I. M. de Andrade, I. Ribeiro, M. T. Bahia, Benznidazole/itraconazole combination treatment enhances anti-*Trypanosoma cruzi* activity in experimental chagas disease. *PLOS ONE* **10**, e0128707 (2015).
26. A. L. Mazzeti, L. d. F. Diniz, K. R. Goncalves, R. S. WonDollinger, T. Assíria, I. Ribeiro, M. T. Bahia, Synergic effect of allopurinol in combination with nitroheterocyclic compounds against *Trypanosoma cruzi*. *Antimicrob. Agents Chemother.* **63**, e02264-18 (2019).
27. S. Khare, A. S. Nagle, A. Biggart, Y. H. Lai, F. Liang, L. C. Davis, S. W. Barnes, C. J. N. Mathison, E. Myburgh, M.-Y. Gao, J. R. Gillespie, X. Liu, J. L. Tan, M. Stinson, I. C. Rivera, J. Ballard, V. Yeh, T. Groessl, G. Federe, H. X. Y. Koh, J. D. Venable, B. Bursulaya, M. Shapiro, P. K. Mishra, G. Spraggon, A. Brock, J. C. Mottram, F. S. Buckner, S. P. S. Rao, B. G. Wen, J. R. Walker, T. Tuntland, V. Molteni, R. J. Glynnne, F. Supek, Proteasome inhibition for treatment of leishmaniasis, Chagas disease and sleeping sickness. *Nature* **537**, 229–233 (2016).
28. R. Moreira da Silva, L. T. Oliveira, N. M. Silva Barcellos, J. de Souza, M. de Lana, Preclinical monitoring of drug association in experimental chemotherapy of Chagas' disease by a new HPLC-UV method. *Antimicrob. Agents Chemother.* **56**, 3344–3348 (2012).
29. L. Perin, R. Moreira da Silva, K. D. Fonseca, J. M. de Oliveira Cardoso, F. A. S. Mathias, L. E. Reis, I. Molina, R. Correa-Oliveira, P. M. Vieira, C. M. Carneiro, Pharmacokinetics and tissue distribution of benznidazole after oral administration in mice. *Antimicrob. Agents Chemother.* **61**, e02410-16 (2017).
30. A. M. C. Canavaci, J. M. Bustamante, A. M. Padilla, C. M. Perez Brandan, L. J. Simpson, D. Xu, C. L. Boehlke, R. L. Tarleton, *In vitro* and *in vivo* high-throughput assays for the testing of anti-*Trypanosoma cruzi* compounds. *PLOS Negl. Trop. Dis.* **4**, e740 (2010).
31. D. Peng, S. P. Kurup, P. Y. Yao, T. A. Minning, R. L. Tarleton, CRISPR-Cas9-mediated single-gene and gene family disruption in *Trypanosoma cruzi*. *MBio* **6**, e02097-14 (2014).
32. K. L. Cummings, R. L. Tarleton, Rapid quantitation of *Trypanosoma cruzi* in host tissue by real-time PCR. *Mol. Biochem. Parasitol.* **129**, 53–59 (2003).
33. D. Xu, C. P. Brandán, M. A. Basombrio, R. L. Tarleton, Evaluation of high efficiency gene knockout strategies for *Trypanosoma cruzi*. *BMC Microbiol.* **9**, 90 (2009).

**Acknowledgments:** We thank J. Nelson from the CTEGD Flow Cytometry Core and M. Kandasamy from the Biomedical Microscopy Core for technical support. We also thank H. Shen, A. Driver, and D. Orr for skillful technical assistance in this work and all the members of Tarleton Research Group for helpful suggestions throughout this study. E. A. Susaki from the University of Tokyo is acknowledged for valuable help regarding tissue clearing protocols.

**Funding:** This work was supported by U.S. NIH grants R01 AI124692 (to R.L.T.) and R21 AI142469 (to R.L.T. and J.M.B.).

**Author contributions:** J.M.B.: conceptualization, formal analysis, investigation, methodology, writing (original draft), and funding acquisition; F.S.-V.: conceptualization, formal analysis, investigation, methodology, and writing (original draft); A.M.P.: conceptualization, formal analysis, investigation, methodology, and writing (review and editing); W.W.: investigation, methodology, and writing (original draft); B.W.: investigation and methodology; R.L.T.: conceptualization, supervision, funding acquisition, methodology, writing (original draft), project administration, and writing (review and editing). J.M.B. performed mice infections, *in vivo* imaging, drug treatment, hemocultures, T cell phenotype, flow cytometry analysis, and perfusion and tissue collection assays. F.S.-V. performed tissue clarification, CLSM imaging, LSFM, and image processing as well as analysis and data acquisition on fluorescence microscopy. A.M.P. performed mice infections, perfusion and tissue collection assays, and analysis of data. W.W. carried out the *in vitro* maximal luminescence ATP detection assay. B.W. performed qPCR and hemoculture.

**Competing interests:** The authors declare that they have no competing interests. **Data and materials availability:** All data associated with this study are present in the paper or the Supplementary Materials.

Submitted 23 April 2020  
Resubmitted 20 July 2020  
Accepted 7 October 2020  
Published 28 October 2020  
10.1126/scitranslmed.abb7656

**Citation:** J. M. Bustamante, F. Sanchez-Valdez, A. M. Padilla, B. White, W. Wang, R. L. Tarleton, A modified drug regimen clears active and dormant trypanosomes in mouse models of Chagas disease. *Sci. Transl. Med.* **12**, eabb7656 (2020).

## A modified drug regimen clears active and dormant trypanosomes in mouse models of Chagas disease

Juan M. Bustamante, Fernando Sanchez-Valdez, Angel M. Padilla, Brooke White, Wei Wang and Rick L. Tarleton

*Sci Transl Med* **12**, eabb7656.  
DOI: 10.1126/scitranslmed.abb7656

### Trouncing trypanosomes

*Trypanosoma cruzi* infection causes Chagas disease in millions of individuals in Latin America, and intensive drug treatment is frequently unsuccessful. Bustamante *et al.* demonstrated that high weekly doses of oral benznidazole over 30 weeks, rather than the current treatment of smaller twice-daily doses over 2 months, resulted in better clearance of both actively replicating and dormant trypanosomes in mouse models of Chagas disease. The clearance of dormant parasites was confirmed by light sheet fluorescence microscopy, which allowed the authors to image whole organs and intact tissues of infected mice. Further studies will determine if this drug regimen will be successful for treating those with Chagas disease.

#### ARTICLE TOOLS

<http://stm.sciencemag.org/content/12/567/eabb7656>

#### SUPPLEMENTARY MATERIALS

<http://stm.sciencemag.org/content/suppl/2020/10/26/12.567.eabb7656.DC1>

#### RELATED CONTENT

<http://stm.sciencemag.org/content/scitransmed/11/519/eaax4204.full>  
<http://stm.sciencemag.org/content/scitransmed/7/310/310ra167.full>  
<http://stm.sciencemag.org/content/scitransmed/7/290/290ra90.full>

#### REFERENCES

This article cites 33 articles, 8 of which you can access for free  
<http://stm.sciencemag.org/content/12/567/eabb7656#BIBL>

#### PERMISSIONS

<http://www.sciencemag.org/help/reprints-and-permissions>

Use of this article is subject to the [Terms of Service](#)

---

*Science Translational Medicine* (ISSN 1946-6242) is published by the American Association for the Advancement of Science, 1200 New York Avenue NW, Washington, DC 20005. The title *Science Translational Medicine* is a registered trademark of AAAS.

Copyright © 2020 The Authors, some rights reserved; exclusive licensee American Association for the Advancement of Science. No claim to original U.S. Government Works